Normal-Mode Analysis of the Glycine Alpha1 Receptor by Three Separate Methods

Edward J. Bertaccini,*,†,‡ James R. Trudell,† and Erik Lindahl§

Department of Anesthesia, Stanford University School of Medicine and Beckman Center for Molecular and Genetic Medicine, Stanford, California 94305-5117, Department of Veterans Affairs, Palo Alto VA Health Care System, Palo Alto, California 94304, and Stockholm Bioinformatics Center and Center for Biomembrane Research, Department of Biochemistry & Biophysics, Stockholm University, Stockholm, Sweden

Received December 22, 2006

Predicting collective dynamics and structural changes in biological macromolecules is pivotal toward a better understanding of many biological processes. Limitations due to large system sizes and inaccessible time scales have prompted the development of alternative techniques for the calculation of such motions. In this work, we present the results of a normal-mode analysis technique based on molecular mechanics that enables the calculation of accurate force-field based vibrations of extremely large molecules and compare it with two elastic network approximate models. When applied to the glycine alpha1 receptor, all three normal-mode analysis algorithms demonstrate an "iris-like" gating motion. Such gating motions have implications for understanding the effects of anesthetic and other ligand binding sites and for the means of transducing agonist binding into ion channel opening. Unlike the more approximate methods, molecular mechanics based analyses can also reveal approximate vibrational frequencies. Such analyses may someday allow the use of protein dynamics elucidated via normal-mode calculations as additional endpoints for future drug design.

INTRODUCTION

We have previously constructed extensive molecular models of glycine alpha1 receptors (GlyRa1) and gamma amino butyric acid receptors (GABAaR) from the superfamily of ligand-gated ion channels (LGICs).[1,2] These models can account for a great deal of the physicochemical and mutational information known about these ion channels. In particular, our models describe a convergence of residues known to be involved in anesthetic effects on these channels, thereby creating a putative anesthetic binding pocket within each of the membrane spanning four-helical bundles.[1−6]

In order to understand the overall gating motion of the LGICs, we have applied normal-mode analyses to such models.[7] Current computational capabilities could allow us to perform full-scale molecular dynamics simulations on a relatively small protein construct to examine larger scale motions in exacting detail. However, to perform large scale molecular dynamics calculations for the microsecond time scales required for actual ion channel opening and closing on a LGIC with approximately 26 000 atoms is intractable, even with the most modern of computational hardware.

Historically, even small proteins were subject to similar limitations 20 years ago, which prompted several groups to develop simplified normal-mode analysis techniques for the examination of the large-scale motions within proteins such as trypsin, lysozyme, crambin, and ribonuclease.[8−10] Normal-mode analysis breaks down the overall motion within a structure into its individual harmonic components.[11−13] It is significantly less computationally demanding, relative to molecular dynamics, and produces reasonable approximations of the larger motions within proteins.

As computational hardware has become more robust, normal-mode analysis on small proteins has mostly given way to more detailed molecular dynamics calculations.[14,15] However, normal-mode analysis is still useful for very large systems and/or slow motions, but a significant problem is that memory and CPU requirements increase as N^2 and N^3, respectively (where N is the number of atoms or groups of atoms in the system). This problem limits the classical molecular dynamics methods to fairly small systems. In the past few years, several groups have developed approximate techniques to work around these limitations for large proteins.[16−21] In particular, the elastic network models have become quite popular for analyses of the growing number of large macromolecular complexes.

Our previous work using the elastic network approximation has demonstrated that one of the highest amplitude motions of our ion channel models is dominated by an "irislike" wringing motion in which the extracellular ligand binding domain (LBD) counter-rotates relative to the transmembrane domain (TMD).[7] However, a difficulty with utilizing such approximations to study the effects of small drug molecules on large-scale receptor motion lies in their inability to account for the subtle effects of individually different atomic interactions. This paper demonstrates our successful implementation and application of a method for full Cartesian normal-mode calculations using a parametrized all-atom molecular mechanics force field[13,22] and compares the results to those obtained by two elastic network models. By using sparse

* Corresponding author phone: (650)493-5000 ext. 65180; fax: (650)-852-3423; e-mail: edwardb@stanford.edu. Corresponding author address: Department of Anesthesia, 112A, Palo Alto VA Health Care System, 3801 Miranda Avenue, Palo Alto, CA 94304.

† Stanford University School of Medicine and Beckman Center for Molecular and Genetic Medicine.

‡ Palo Alto VA Health Care System.

§ Stockholm University.

10.1021/ci600566j CCC: $37.00
Published on Web 06/30/2007

matrix representations, we are able to retain all degrees of freedom but still keep the memory requirements modest—in fact they are proportional to the number of atoms. As an example, we have calculated the lowest-frequency normal modes of an entire LGIC model containing more than 26 000 atoms by all three methods.

METHODS

Construction of the GlyRa1 Model. The sequence of the human GlyRa1 was obtained from the National Center for Biotechnology and Information. It was edited so as to contain only the mature sequence without precursor amino acids. It was also edited so as to contain an abbreviated version of the TM3-4 loop composed of only 9 native residues from the loop region itself along with a chain of 5 glycine residues substituted for the central remaining bulk of the loop. The human GABAaR and the GlyRa1 have approximately 69% sequence similarity and nearly 34% sequence identity. We therefore utilized the coordinates of the homomeric GABARa1 pentamer complex from our previous work,[1,7] composed of both an extracellular ligand-binding domain and a transmembrane domain, as a template within the Modeler module of InsightII 2005. The edited sequence of the mature GlyRa1 was threaded onto this template so as to provide an initial homology model for each GlyRa1 subunit. All five GlyRa1 subunits were then merged into one coordinate file based on the symmetry of the template, thereby producing the symmetric pentameric structure of the whole LGIC. The first 10 and the last 8 residues of the GlyRa1 subunits were poorly mapped and thus edited out. Using the CVFF force field and the Discover_3 molecular mechanics module, hydrogens were then added to the homology model structure, and an autorotamer check was performed to initially optimize amino acid side-chain conformations. After tethering the protein backbone with a force constant of 100 kcal/mol-Å^2, the entire complex was further optimized using the steepest descents algorithm to a gradient of 1000 kcal/mol-Å followed by a conjugate gradient algorithm to a gradient of 1 kcal/mol-Å. This model was used for the subsequent three different types of normal-mode calculations.

Normal-Mode Analysis. The theoretical foundation of normal-mode analysis is to provide a simplified description of the motion of an N-particle system about a local minimum within the potential energy landscape. We examined three algorithms for the calculation of the normal modes of the GlyRa1 model: ElNemo, LAABEN, and GROMACS.

ElNemo Approximation for Elastic Network Normal-Mode Analyses. The PDB formatted version of the GlyRa1 model was submitted for normal-mode calculation based on the ElNemo approximate method.[12] These elastic network modes are only based on alpha carbon coordinates and proximity in space, although all atomic coordinates are regenerated in the output by using rotation-translation blocks.[23] Input parameters included the request for the first 5 nontrivial normal modes, a DQMIN to DQMAX range of −500 to 500, and a DQSTEP of 50. The NRBL setting was set to "auto", and the default cutoff of 8 residues was used to identify elastic interaction ranges.

Lindahl All-Atom Based Elastic Network (LAABEN) Normal-Mode Analyses. After hydrogens were added to the PDB formatted version of the GlyRa1 model, it was submitted for normal-mode calculation via the method of Lindahl[11,24] as described in our previous work[7] and run locally on a Dell Precision 670 Workstation running 32 bit RedHat Linux WS 3.0. This, too, is an elastic network algorithm we have previously implemented, but it retains all atomic coordinates in the normal-mode calculation and uses a sparse matrix representation of the Hessian matrix to limit memory requirements. Input parameters included the total number of normal modes to be generated (including the six rigid-body motions of the whole complex) at 11, an interaction distance weight parameter of 2 Å, and an interaction cutoff default of 10 Å.

All-Atom Fully Parametrized Cartesian Molecular Mechanics Based Normal-Mode Analyses Using GROMACS Version 3.3.1. Finally, we have implemented the all-atom force field based normal-mode algorithm in GROMACS by using sparse matrix storage both for the Hessian matrix and during the diagonalization step.[25] Traditionally, the huge number of degrees of freedom for Cartesian systems combined with memory requirements that grow as *N*N* (where *N* is the number of atoms or groups of atoms in the system) has inhibited normal-mode analysis for large systems. Innovative techniques such as using molecular symmetry[26] provide solutions for some systems but do not change the fundamental scaling behavior. In contrast, sparse matrix storage means that the memory requirements are only proportional to the number of atoms, and as long as only a handful of low-frequency modes are required, it enables large system normal-mode analysis with very modest hardware requirements. Starting with the GROMACS 3.3.1 distribution, this sparse storage normal-mode analysis algorithm is now used by default whenever possible. The only serious limitation is that it relies on a cutoff outside of which atoms do not interact (thus the sparse property), and hence it cannot be used with lattice summation algorithms such as particle mesh Ewald methods.[27] Such sparse matrix methods have been previously used by others for analyses of macromolecules[28,29] and, as noted below, have been subjected to similar limitations related to cutoff effects.[29,32]

The PDB formatted version of the GlyRa1 model was prepared for normal-mode calculation by using the OPLS-AA/L all-atom molecular mechanics force field[22] in GROMACS[13] and locally run on a Dell Precision 670 Workstation. In contrast to the elastic network models, force field based normal-mode analysis requires careful energy minimization of the initial structure. Nonbonded electrostatics and van der Waals interactions were treated with cutoffs at 10 Å, smoothly switched to zero between 8 Å and 10 Å. Initial optimization was with a steepest descent algorithm to a gradient of 1000 kcal/mol-Å, followed by a conjugate gradient algorithm to a gradient of 10 kcal/mol-Å, and finally by low memory BFGS optimization to a gradient of 1 kcal/mol-Å. Final optimization to the limit of machine precision was performed using the low memory BFGS minimizer (typically $<10^{-6}$ kcal/mol-Å). Finally, normal-mode analysis was performed using the algorithm in GROMACS.

Since it is known that truncation of long-range nonbonded terms can affect the results of normal-mode calculations,[29−32] additional trials of optimizations were performed using cutoff schemes smoothly switched to zero between 6 Å and 8 Å, between 10 Å and 12 Å, and a wider switching region from 8 Å to 12 Å. Finally interaction functions that are modified

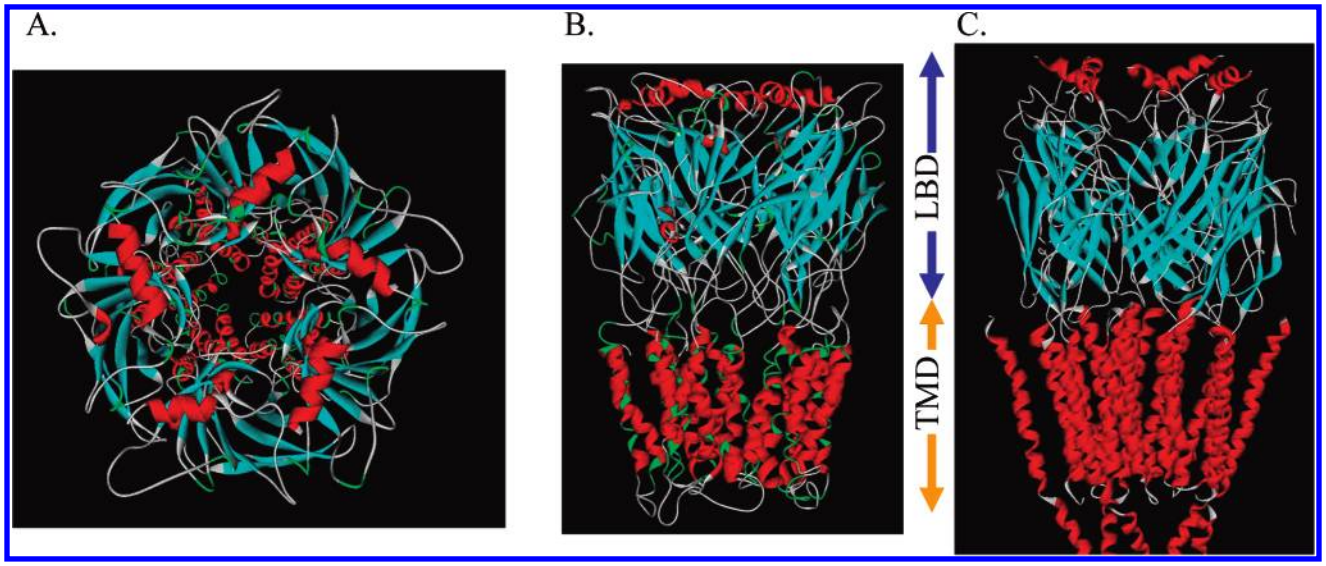

Figure 1. The transverse (A) and longitudinal (B) cross-sectional images of our model. Note the existence of a continuous channel traversing the entire length of the complex that would function as the ion pore passageway. (C) The nAChR model of Unwin (PDB id 2BG9). Despite construction by a completely different means, comparison of parts B (our model of the glyRa1) and C (Unwin's model of the nAChR) demonstrate the striking similarity of the two models of LGICs (LBD = ligand binding domain, TMD = transmembrane domain).

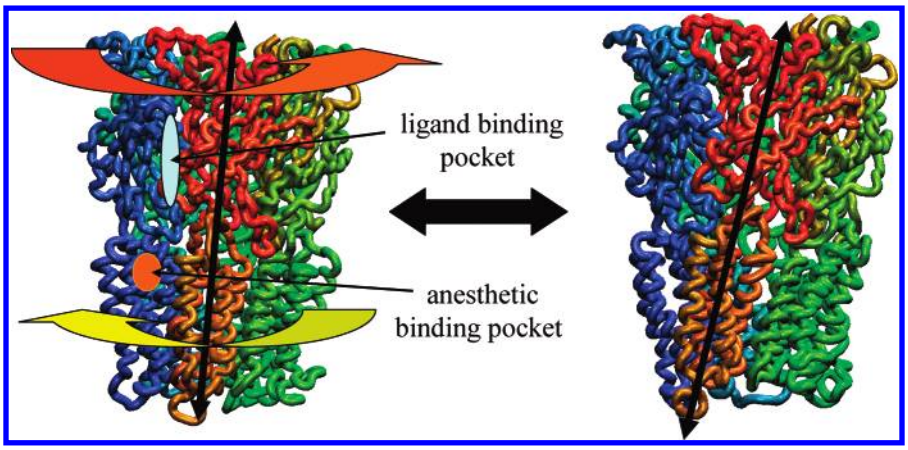

Figure 2. The lowest frequency, highest amplitude motion as seen in the first nontrivial normal mode within the GlyRa1 calculated using GROMACS is consistent with ion channel gating. It is represented as an "iris-like" wringing motion characterized by simultaneous axially symmetric twisting motions of the LBD in the opposite direction to those of the TMD.

by switching/shifting the force rather than the potential[13,32,33] were additionally implemented to avoid the unnatural force increase associated with the classical potential energy switch function.

Analyses of Data. Each of the aforementioned normal-mode calculations produced coordinate trajectory files for analysis. Root-mean-square deviations (rmsd) of each residue were produced either from the original program itself (ElNemo) or from the application of the rmsd analysis utility within GROMACS to the coordinate trajectory files output from the remaining normal-mode analyses (LAABEN and GROMACS). The rmsd data were then imported into Microsoft Excel for plotting and further analysis of the overall similarity of motion between the three different normal-mode calculations.

RESULTS

Our model of the GlyRa1 demonstrates that the β sheet structures of the LBD modeled on the AChBP template were preserved. Additionally, and despite years of controversy,[34,35] the TMD clearly demonstrates its overall form as a pentamer of four-helical bundles arranged around a central ion pore. This structural motif can be seen in transverse cross-sectional (Figure 1A) and longitudinal (Figure 1B) images of our model and is very consistent with the cryoelectron microscopy results of Unwin (Figure 1C).[36,37] This motif was also readily seen in a formal Ramachandran analysis. There is a continuous channel traversing the entire length of the complex that functions as the ion pore.

The lowest frequency, highest amplitude motion from each method of normal-mode calculation is consistent with ion channel gating. It is represented as an "iris-like" wringing motion, as one might wring water from a washcloth in opposite directions when gripping from opposite ends (Figure 2). This motion may be responsible for part of the axially symmetric opening and closing motions of the ion channel pore.

A plot of the rmsd of the individual alpha carbon atoms over the entire GlyRa1 complex for all three methods of normal-mode calculation is strikingly similar. This similarity can be seen in Figure 3, where the rmsd of the alpha carbons calculated with the ElNemo method are in dark blue, those

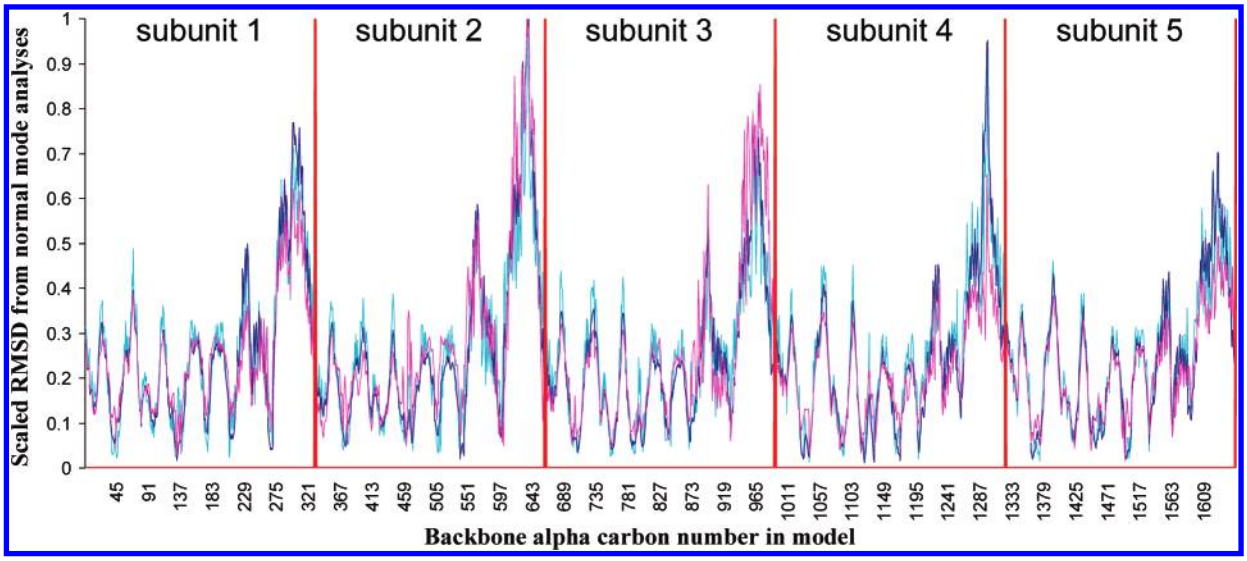

Figure 3. Plot of the rmsd of the alpha carbons within the GlyRa1 vs the residue number within the model across all 5 subunits for each method of normal-mode calculation. The rmsds calculated via the EINemo method are in dark blue, those from the LAABEN method are in cyan, and those calculated via the GROMACS method are in pink. They have been scaled to represent the proportion of the maximum rmsd for a given technique so as to be plotted on the same graph. Individual subunit limits are denoted by the vertical red lines.

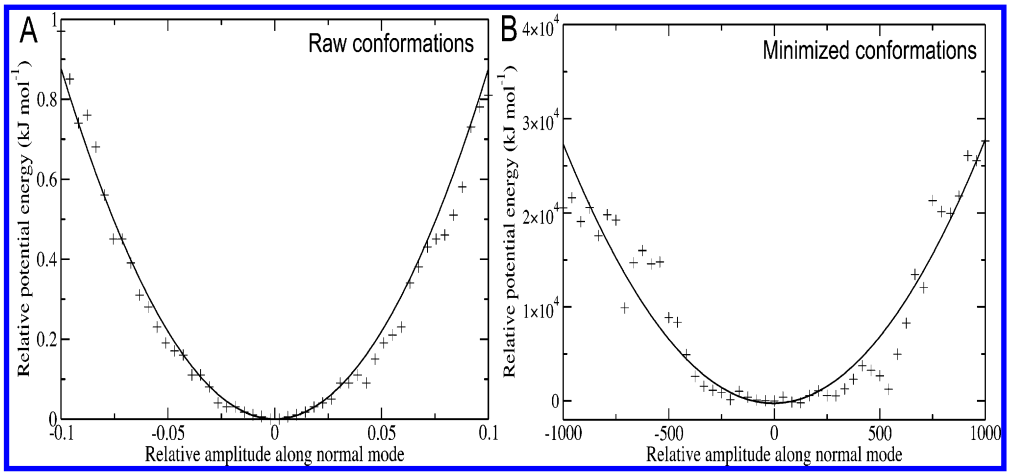

Figure 4. (A) Energy variation of structures along the lowest nontrivial normal mode. The mode amplitudes here correspond to displacements of only 0.001 Å, i.e. van der Waals contacts cause unrealistically high energies. Second derivative (not mass-weighted) ($k = 0.877$ kJ/(mol $\times$ Å^2). (B) Energy variation after energy minimization of structures, mode amplitudes corresponds to displacements up to 6 Å. With a second derivative of ($k = 0.000275$ kJ/(mol $\times$ Å^2) the relative scaling would lead to an eigenvalue almost 3200 times lower, and a frequency 60 times lower than the raw result, or a period in the range of 200 ps.

with the LAABEN method are in cyan, and those calculated with the GROMACS method are in pink. The values have been scaled to represent the proportion of the maximum rmsd for a given technique so as to be plotted on the same graph.

The harmonic vibration frequency of this motion can only be directly calculated from the GROMACS molecular mechanics based method.[13] This first nontrivial, lowest frequency, highest amplitude motion is characterized by a wavenumber of 9.3 cm^{-1}. This translates into a frequency of vibration of approximately 279 GHz or 3.6 ps per cycle.

This frequency range is much faster than that derived from electrophysiologic analyses of ion channel gating time scales. The reason for this is that any normal-mode approach relies on a pointwise harmonic approximation to the energy landscape around the local minimum. Since atoms are not free to relax when the structure is moved along a normal-mode vector, bad van der Waals contacts and bond/angle distortion will lead to unrealistic energies even when the structure cRMS is still within picometers of the minimum, and thus eigenfrequencies that are too high (Figure 4a) can be generated. To compensate for this possible frequency overestimation and determine more realistic energy variations for this amount of distortion, we extracted 50 conformations along the motion vector corresponding to cRMS values up to 6 Å. These conformations were all additionally minimized with 10 000 steps of low memory BFGS optimization. Since these minimizations were performed with full Cartesian degrees of freedom (rather than along the mode), the structures did not move significantly back toward the normal-mode minimum (average cRMS change during minimization was 0.6 Å). The minimizations removed bad local contacts and bond deformations, which resulted in the smaller energy variations shown in Figure 4b. Due to mass-weighting it is nontrivial to extract normal-mode frequencies directly from Figure 4b. However, since the frequency is proportional to the square root of the eigenvalue, which in turn is proportional to the second derivative, we can estimate a change in frequency between parts a and b of Figure 4. The relative

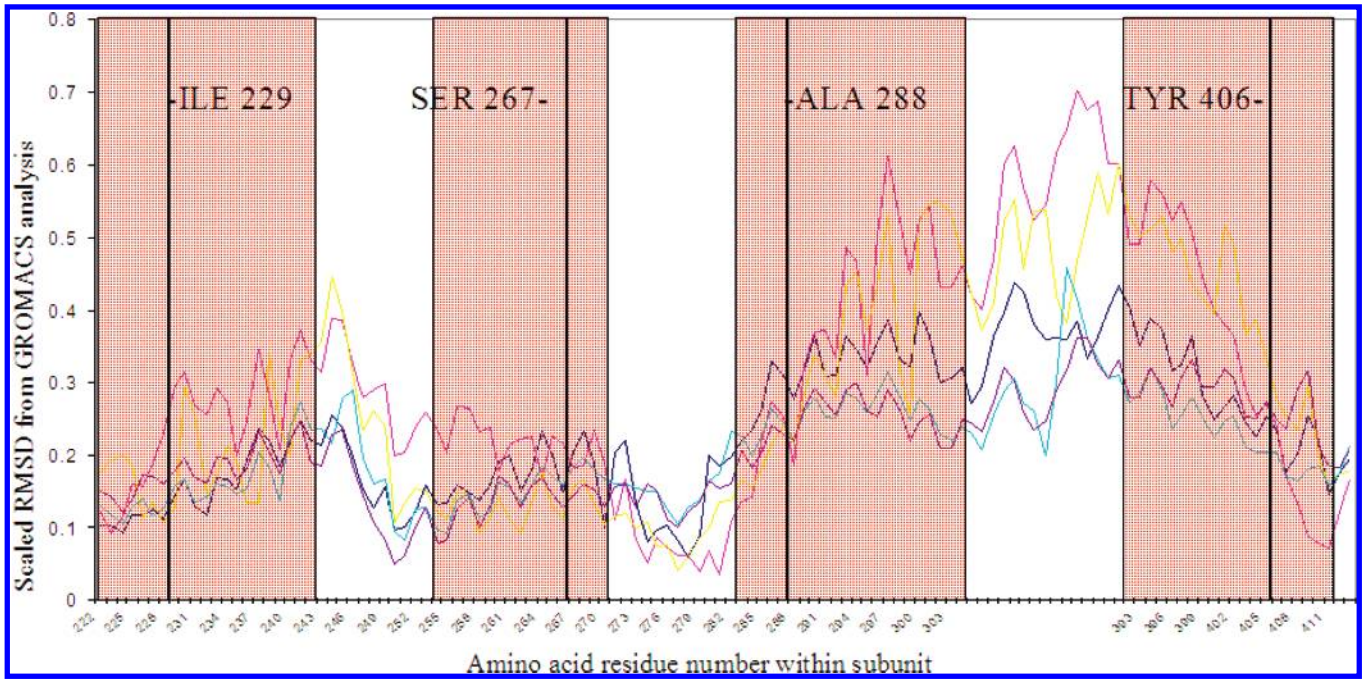

Figure 5. Plot of the rmsd of the alpha carbons within the GlyRa1 vs actual amino acid residue number calculated using the GROMACS method. The red block regions denote the previously predicted limits of the alpha helical regions. Those residues previously associated with the alteration of anesthetic effects on glyRa1 function (ILE 229, SER 267, ALA 288, and the postulated TYR 406 denoted by the solid lines within the alpha helical regions) converge on a common cavity within the TMD region of the individual subunits. These putative anesthetic binding sites lie within the outer third of the four-helix bundles. The plot of the rmsd of these residues during channel gating demonstrates that the anesthetic binding pocket seems to be located in a region of a somewhat intermediate motion. Five separate colors represent each of the 5 separate alpha subunits within the pentameric homomer.

change in second derivative between the raw and energy-minimized normal-mode vibration corresponds approximately to a correction factor of 60 to the frequency. This would imply a time period closer to 200 ps per cycle, although the primary conclusion is that larger distortions are energetically possible.

It is an interesting question to what extent these results can be trusted quantitatively. First, as shown by Janezic and Brooks[29−32] it is clear that normal-mode frequencies depend on the interaction setup used. Indeed, merely altering the cutoff produces wavenumbers ranging from 8.1 cm^{-1} (6/8 Å switch) to 12.4 cm^{-1} (10/12 Å). When the switch region is expanded to 8−12 Å to reduce the artificially increased force, the wavenumber drops to 3.9 cm^{-1}. It gets even lower (2.0 cm^{-1}) when the force rather than potential is switched in the 8−12 Å range according to the GROMACS force switching function.[13] Switching the force over the entire 0−12 Å region results in a somewhat higher wavenumber (2.4 cm^{-1}). These differences are likely due both to the different steepness/smoothness of the interaction potentials as well as the structure obtained in the energy minimization. Although they are all within an order of magnitude, even larger differences could plausibly be seen had it been possible to calculate modes without cutoffs for this structure.[29−31] Even then, such calculations would be done in vacuo, which is, at best, a rough approximation of a protein in a membrane/water environment where the real motions are heavily dampened by the solvent.[38−40] However, while frequencies are only order-of-magnitude estimates, the overall shape of the normal mode seems much less dependent on the methodology and interaction potentials, for instance, as seen in comparisons with Essential Dynamics (ED) simulations in water.[40,41]

For the present system, all the additional setups with different potential or force switching cutoffs produce a first nontrivial mode whose motion maintains a twist extremely similar to that produced by the 8 Å/10 Å scheme as demonstrated in both a quantitative comparison through scalar product analysis as well as an overall three-dimensional visual qualitative examination. Relative to the 8/10 Å system, the scalar product of the normal-mode vectors for both the 6/8 Å switch and 10/12 Å switch is 0.90, while it is slightly lower at 0.86 for the wider 8/12 Å switch. With force switching from 8 to 12 Å the same scalar product is 0.89 and finally 0.87 when switching the force from 0 Å. Thus, just as reported by Rueda,[41] the shape of motions appears to be quite insensitive to details and initial energy minimization and clearly more reliable than the absolute frequencies quoted.

Those residues associated with the alteration of anesthetic effects on GlyRa1 function (ILE 229, SER 267, and ALA 288), as demonstrated from previous experiments, converge on a common cavity within the TMD region of the individual subunits.[1−6,42] These putative anesthetic binding sites lie within the extracellular third of the TMD four-helical bundles. A plot of the rmsd of these TMD residues during motion demonstrates that the putative anesthetic binding pocket seems to be consistently located in a region of intermediate motion (Figure 5).

The transduction of native ligand binding from the extracellular LBD to the TMD occurs via two methods of coupling: The first means is by way of the protein backbone as the amino acid sequence transitions from the LBD to the TMD at Gly 221. The second means is through the intercalation of the TMD2-3 loop with loops 2 and 7 from the LBD[43] (Figure 6).

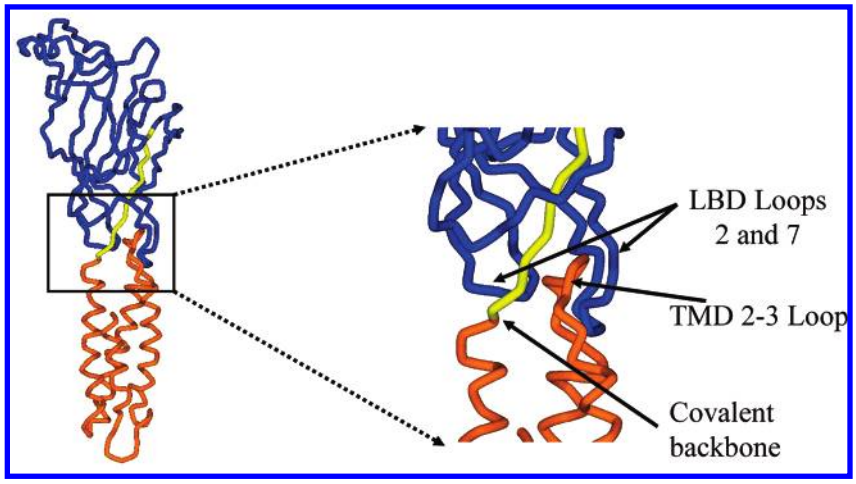

Figure 6. The transduction of native ligand binding from the extracellular LBD to the TMD within a single subunit occurs via two methods of coupling. The first means is by way of the covalent bonds of the protein backbone as the amino acid sequence transitions from the pre-TM1 region of the LBD (yellow) to TMD (orange) at glycine 221. The second means is through the intercalation of the TMD2-3 loop (orange) with loops 2 and 7 (blue) from the LBD.

DISCUSSION

We have constructed molecular models of LGICs that can account for a great deal of the physicochemical and mutational information known about these channels. Our current model of a human GlyRa1 homomer demonstrates several of these key findings. The extracellular LBD has a large component of β sheet structure. Glycine is thought to bind at the interface between the subunits of this region. This LBD mates well with a model of the TMD built by completely independent means. The transmembrane domain is composed of a pentamer of tetrameric alpha helical bundles, within which is a putative anesthetic binding site. These sites illustrate the convergence of residues known to be involved in anesthetic effects on these ion channels.[2,5,42] The diameter of the pore channel is large enough to accommodate ion passage. The residues involved in the ion selectivity filter are located near the intracellular end of the TMD pore. While our model was developed by knowledge-based homology modeling, the overall protein construct is extremely similar to the model of the homologous nicotinic acetylcholine receptor (PDB ID 2BG9) within *Torpedo californicus* derived from the cryoelectron microscopy of Nigel Unwin (Figure 1C).[36,37]

There are now numerous studies to suggest that anesthetics may produce their effect by direct interaction with protein targets well-known to be involved in the transmission of information within the central nervous system.[1−6,42] With a putative anesthetic binding site identified, it has been our eventual goal to seek how anesthetic binding, and many other ligands for that matter, may alter overall ion channel function. However, modeling the large scale motions of LGICs consisting of approximately 26 000 atoms using traditional molecular dynamics calculations over millisecond time scales is intractable, even with the most modern of computational hardware.[15] Therefore, we implemented the far more efficient methods of normal-mode analyses to assess the large scale gating motions of these proteins.

Since the natural function of LGICs is the gating motion involved in the transition from the resting to the open state, we postulated that such a natural function should be represented in the harmonic motion of some of the highest amplitude and lowest frequency normal-mode vibrations. Our initial analyses utilized an elastic network approximation[12] involving groups of adjacent amino acids. Elastic network models treat every bonded atom as an equivalent ball separated by a spring of equal tension. We subsequently extended and reproduced this result with a more detailed all-atom elastic network model developed by Lindahl and Delarue.[24] This motion was initially demonstrated in the "iris-like" wringing motion within our model of a GABARa1 homomer.[7] Concurrent with our work, several other groups have used normal-mode analysis to calculate similar "twisting" motions in the nAChR,[18,19] the potassium channel,[20] and the bacterial mechanosensitive channel (MSCL).[21] These studies not only have further served to validate the implementation of such techniques but also aided in the validation of our model construct and its overall motion. However, preliminary calculations performed in our laboratory have suggested that using such elastic network approximations demonstrates little or no effect of point mutations or small bound ligands/drugs on the large-scale motions associated with channel gating. This lack of effect may be due to the coarse-grained nature of the elastic network approximations. That is, the process of representing all of the atoms for groups of amino acid residues as nonvariable units devoid of individualized atomic parametrization and interactions may under represent the otherwise subtle effects of electrostatic or van der Waals interactions between protein and ligand.

This lack of ligand-induced changes with the elastic network algorithms prompted our efforts to demonstrate the practicality of using a more rigorous technique for normal-mode analysis, as described in this paper. By many benchmarks, GROMACS is an extremely fast and efficient molecular mechanics software package.[13] We made use of its extensive abilities and uniquely programmed libraries for the optimization and calculation of the normal modes of our GlyRa1 model. We have now successfully calculated the normal-mode vibrations of our large LGICs using the detailed, all-atom, full-scale molecular mechanics force field present within GROMACS (OPLS-AA/L).[22] Such calculations take many hours to a few days to complete, as opposed to the several hours required for the elastic network models.

However, the more detailed calculation takes into account not only differential atomic identities but also differential interatomic interactions.

This technique clearly reproduces the natural harmonic wringing motion associated with ion channel gating as the largest amplitude, lowest frequency normal mode. It also demonstrates the potential for transducing ligand binding effects within the extracellular LBD into ion channel opening in the distant TMD. The results are consistent with all of our previous analyses, but such detailed methods now yield several additional advantages.

GROMACS based normal-mode calculations allow the calculation of an approximate frequency of vibration. While ion channel gating appears to occur on the microsecond time scale as noted by electrophysiologic analyses, many functional protein motions occur on the order of 10^{-6}−10^{-12} s.[15] Our normal-mode calculations reveal a subnanosecond time scale (10^{-10}) for the wringing motion associated with channel gating within the LGICs, well within the aforementioned range for protein motions.

Even with such detailed calculations, there may be potential sources of refinement to the vibration frequency presented. Our current normal-mode calculations were carried out in vacuo and without the presence of either the natural hydration shell around the LBD[33,44] or the lipid bilayer around the TMD.[45] While still the goal of future computations, the presence of such additional components could readily dampen such vibrations and bring the normal-mode time scale much closer to that which is electrophysiologically observed. Additionally, while the raw frequency reported includes the local bond/angle deformation as part of the global structural rearrangements, it is partly possible to minimize this local effect in postprocessing. This can be accomplished either by ignoring the corresponding potential energy terms or by reapplying energy minimization to sequential frames from the normal-mode trajectory as was done in this paper (Figure 4).

Normal-mode analyses may also aid in the determination of various conformational states of an ion channel. Some groups have used this notion to suggest the open state of an ion channel.[18−20] Such estimations have been primarily based on the determination of which frame in the vibrational trajectory is characterized by an ion channel diameter capable of accommodating an ion of a given radius. However, such analysis is limited by the currently undetermined differential hydration state of many ions as they pass through the ion channel for the variety of ion pore proteins within the family of LGICs. This ionic radius would have great bearing on the pore diameter at given points within the channel that would be necessary for ion passage, as shown in recent work on the potassium channel[46] and the nAChR.[47]

Normal-mode analyses using full molecular mechanics force fields may also aid in future drug design. There are currently a great many ways of performing high throughput screening of various drug candidates based upon both ligand and receptor derived pharmacophore information. However, it seems quite reasonable that if the collective protein motions associated with a specific function and/or drug binding can be discerned from detailed normal-mode analyses, this could provide additional selection criteria in the final stages of lead refinement and a computational search for effective new therapeutic agents.

ACKNOWLEDGMENT

This work was supported by the Department of Veterans Affairs, the Stanford University School of Medicine, and the National Institutes of Health grants GM064371 and AA013378.

Supporting Information Available: Coordinates of our most recent model of the glyRa1 as well as two movies of the first nontrivial normal-mode vibration. This material is available free of charge via the Internet at http://pubs.acs.org.

REFERENCES AND NOTES

(1) Trudell, J. R.; Bertaccini, E. Comparative modeling of a GABAA a1 receptor using three crystal structures as templates. *J. Mol. Graphics Modell.* **2004**, *23*, 39−49.
(2) Bertaccini, E.; Shapiro, J.; Brutlag, D.; Trudell, J. R. Homology modeling of a human glycine alpha 1 receptor reveals a plausible anesthetic binding site. *J. Chem. Inf. Model.* **2005**, *45*, 128−135.
(3) Yamakura, T.; Bertaccini, E.; Trudell, J. R.; Harris, R. A. Anesthetics and ion channels: molecular models and sites of anesthetic action. *Ann. Rev. Pharmacol. Toxicol.* **2001**, *41*, 23−51.
(4) Bertaccini, E.; Trudell, J. R. Molecular modeling of the transmembrane regions of ligand-gated ion channels: Progress and Challenges. *Int. Rev. Neurobiol.* **2001**, *48*, 141−166.
(5) Jenkins, A.; Greenblatt, E. P.; Faulkner, H. J.; Bertaccini, E.; Light, A.; Lin, A.; Andreasen, A.; Viner, A.; Trudell, J. R.; Harrison, N. L. Evidence for a common binding cavity for three general anesthetics within the GABAA receptor. *J. Neurosci.* **2001**, *21*, RC136.
(6) Trudell, J. R.; Bertaccini, E. Molecular modelling of specific and non-specific anaesthetic interactions. *Br. J. Anaesth.* **2002**, *89*, 32−40.
(7) Bertaccini, E.; Trudell, J. R.; Lindahl, E. Normal mode analysis reveals the channel gating motion within a ligand gated ion channel model. *Int. Congr. Ser.* **2005**, *1283*, 160−163.
(8) Brooks, B. R.; Karplus, M. Harmonic dynamics of proteins: normal modes and fluctuations in bovine pancreatic trypsin inhibitor. *Proc. Natl. Acad. Sci. U.S.A.* **1983**, *80*, 6571−6575.
(9) Go, N.; Noguti, T.; Nishikawa, T. Dynamics of a small globular protein in terms of low-frequency vibrational modes. *Proc. Natl. Acad. Sci. U.S.A.* **1983**, *80*, 3696−3700.
(10) Levitt, M.; Sander, C.; Stern, P. S. Protein normal-mode dynamics: trypsin inhibitor, crambin, ribonuclease and lysozyme. *J. Mol. Biol.* **1985**, *181*, 423−447.
(11) Delarue, M.; Sanejouand, Y. H. Simplified normal mode analysis of conformational transitions in DNA-dependent polymerases: the elastic network model. *J. Mol. Biol.* **2002**, *320*, 1011−1024.
(12) Suhre, K.; Sanejouand, Y. H. ElNemo: a normal mode web server for protein movement analysis and the generation of templates for molecular replacement. *Nucleic Acids Res.* **2004**, *32*, W610−W614.
(13) van der Spoel, D.; Lindahl, E.; Hess, B.; Groenhof, G.; Mark, A. E.; Berendsen, H. J. GROMACS: fast, flexible, and free. *J. Comput. Chem.* **2005**, *26*, 1701−1718.
(14) Rhee, Y. M.; Sorin, E. J.; Jayachandran, G.; Lindahl, E.; Pande, V. S. Simulations of the role of water in the protein-folding mechanism. *Proc. Natl. Acad. Sci. U.S.A.* **2004**, *101*, 6456−6461.
(15) Karplus, M.; McCammon, J. A. Molecular dynamics simulations of biomolecules. *Nat. Struct. Biol.* **2002**, *9*, 646−652.
(16) Tama, F.; Valle, M.; Frank, J.; Brooks, C. L., III. Dynamic reorganization of the functionally active ribosome explored by normal mode analysis and cryo-electron microscopy. *Proc. Natl. Acad. Sci. U.S.A.* **2003**, *100*, 9319−9323.
(17) Atilgan, A. R.; Durell, S. R.; Jernigan, R. L.; Demirel, M. C.; Keskin, O.; Bahar, I. Anisotropy of fluctuation dynamics of proteins with an elastic network model. *Biophys. J.* **2001**, *80*, 505−515.
(18) Taly, A.; Delarue, M.; Grutter, T.; Nilges, M.; Le Novere, N.; Corringer, P. J.; Changeux, J. P. Normal mode analysis suggest a quaternary twist model for the nicotinic receptor gating mechanism. *Biophys. J.* **2005**, *88*, 3954−3965.
(19) Cheng, X.; Lu, B.; Grant, B.; Law, R. J.; McCammon, J. A. Channel opening motion of alpha7 nicotinic acetylcholine receptor as suggested by normal mode analysis. *J. Mol. Biol.* **2006**, *355*, 310−324.
(20) Shen, Y.; Kong, Y.; Ma, J. Intrinsic flexibility and gating mechanism of the potassium channel KcsA. *Proc. Natl. Acad. Sci. U.S.A.* **2002**, *99*, 1949−1953.
(21) Valadie, H.; Lacapcre, J. J.; Sanejouand, Y. H.; Etchebest, C. Dynamical properties of the MscL of Escherichia coli: a normal mode analysis. *J. Mol. Biol.* **2003**, *332*, 657−674.
(22) Kaminski, G. A.; Friesner, R. A.; Tirado-Rives, J.; Jorgensen, W. L. Evaluation and reparametrization of the OPLS-AA force field for proteins via comparison with accurate quantum chemical calculations on peptides. *J. Phys. Chem. B* **2001**, *105*, 6474−6487.

(23) Tama, F.; Gadea, F. X.; Marques, O.; Sanejouand, Y. H. Building-block approach for determining low-frequency normal modes of macromolecules. *Proteins* **2000**, *41*, 1−7.
(24) Lindahl, E.; Azuara, C.; Koehl, P.; Delarue, M. NOMAD-Ref: visualization, deformation and refinement of macromolecular structures based on all-atom normal mode analysis. *Nucleic Acids Res.* **2006**, *34*, W52−W56.
(25) Lehoucq, R. B.; Sorensen, D. C.; Yang, C. *ARPACK Users' guide: Solution of large-scale eigenvalue problems with implicitly restarted Arnoldi methods;* SIAM: Philadelphia, PA, 1998; pp 1−160.
(26) van Vlijmen, H. W.; Karplus, M. Normal mode calculations of icosahedral viruses with full dihedral flexibility by use of molecular symmetry. *J. Mol. Biol.* **2005**, *350*, 528−542.
(27) Essman, U.; Perela, L.; Berkowitz, M. L.; Darden, T.; Pedersen, L. G. A smooth particle mesh Ewald method. *J. Chem. Phys.* **1995**, *103*, 8577−8592.
(28) Li, G.; Cui, Q. A Coarse-Grained Normal Mode Approach for Macromolecules: An Efficient Implementation and Application to Ca2+-ATPase. *Biophys. J.* **2002**, *83*, 2457−2474.
(29) Janezic, D.; Brooks, B. R. Harmonic analysis of large systems. II. Comparison of different protein models. *J. Comput. Chem.* **1995**, *16*, 1543−1553.
(30) Janezic, D.; Venable, R. M.; Brooks, B. R. Harmonic analysis of large systems. III. Comparison with molecular dynamics. *J. Comput. Chem.* **1995**, *16*, 1554−1566.
(31) Brooks, B. R.; Janezic, D.; Karplus, M. Harmonic analysis of large systems. I. Methodology. *J. Comput. Chem.* **1995**, *16*, 1522−1542.
(32) Steinbach, P. J.; Brooks, B. R. New spherical-cutoff methods for long-range forces in macromolecular simulation. *J. Comput. Chem.* **1994**, *15*, 667−683.
(33) Steinbach, P. J.; Brooks, B. R. Protein hydration elucidated by molecular dynamics simulation. *Proc. Natl. Acad. Sci. U.S.A.* **1993**, *90*, 9135−9139.
(34) Bertaccini, E.; Trudell, J. R. Predicting the transmembrane secondary structure of ligand-gated ion channels. *Protein Eng.* **2002**, *15*, 443−453.
(35) Unwin, N. Nicotinic acetylcholine receptor at 9 A resolution. *J. Mol. Biol.* **1993**, *229*, 1101−1124.
(36) Miyazawa, A.; Fujiyoshi, Y.; Unwin, N. Structure and gating mechanism of the acetylcholine receptor pore. *Nature* **2003**, *423*, 949−955.
(37) Unwin, N. Refined structure of the nicotinic acetylcholine receptor at 4A resolution. *J. Mol. Biol.* **2005**, *346*, 967−989.
(38) Hinsen, K.; Thomas, A.; Field, M. J. Analysis of domain motions in large proteins. *Proteins* **1999**, *34*, 369−382.
(39) Hinsen, K. Analysis of domain motions by approximate normal mode calculations. *Proteins* **1998**, *33*, 417−429.
(40) Amadei, A.; Linssen, A. B.; Berendsen, H. J. Essential dynamics of proteins. *Proteins* **1993**, *17*, 412−425.
(41) Rueda, M.; Chacon, P.; Orozco, M. Thorough Validation of Protein Normal Mode Analysis: A Comparative Study with Essential Dynamics. *Structure* **2007**, *15*, 565−575.
(42) Mihic, S. J.; Ye, Q.; Wick, M. J.; Koltchine, V. V.; Krasowski, M. D.; Finn, S. E.; Mascia, M. P.; Valenzuela, C. F.; Hanson, K. K.; Greenblatt, E. P.; Harris, R. A.; Harrison, N. L. Sites of alcohol and volatile anaesthetic action on GABA(A) and glycine receptors. *Nature* **1997**, *389*, 385−389.
(43) Kash, T. L.; Jenkins, A.; Kelley, J. C.; Trudell, J. R.; Harrison, N. L. Coupling of agonist binding to channel gating in the GABAA receptor. *Nature* **2003**, *421*, 421−425.
(44) Azuara, C.; Lindahl, E.; Koehl, P.; Orland, H.; Delarue, M. PDB-_Hydro: incorporating dipolar solvents with variable density in the Poisson-Boltzmann treatment of macromolecule electrostatics. *Nucleic Acids Res.* **2006**, *34*, W38−W42.
(45) Hofsass, C.; Lindahl, E.; Edholm, O. Molecular dynamics simulations of phospholipid bilayers with cholesterol. *Biophys. J.* **2003**, *84*, 2192−2206.
(46) Doyle, D. A.; Cabral, J. M.; Pfuetzner, R. A.; Kuo, A.; Gulbis, J. M.; Cohen, S. L.; Chait, B. T.; MacKinnon, R. The structure of the potassium channel: molecular basis of K^+ conduction and selectivity. *Science* **1998**, *280*, 69−77.
(47) Beckstein, O.; Biggin, P. C.; Sansom, M. S. P. A hydrophobic gating mechanism for nanopores. *J. Phys. Chem. B* **2001**, *105*, 12902−12905.

CI600566J